Capture of CO_2 from Combustion Gases in a Fluidized Bed of CaO

J. Carlos Abanades
Dep. Energy and Environment, Instituto de Carboquímica (CSIC), Miguel Luesma 4, 50015 Zaragoza, Spain

Edward J. Anthony, Dennis Y. Lu, and Carlos Salvador
CANMET Energy Technology Centre, Natural Resources Canada; 1 Haanel Drive, Ottawa ON, K1A 1M1 Canada

Diego Alvarez
INCAR (CSIC), C/Francisco Pintado Fe, No. 26, 33011 Oviedo, Spain

DOI 10.1002/aic.10132
Published online in Wiley InterScience (www.interscience.wiley.com).

Experiments in a pilot-scale fluidized-bed reactor have been carried out to investigate the carbonation reaction of CaO, as a potential method for CO_2 capture from combustion flue gases at high-temperatures. Results show that CO_2 capture efficiencies are very high, while there is a sufficient fraction of CaO in the bed reacting in the fast reaction regime. The total capture capacity of the bed decays with the number of carbonation-calcination cycles. The experimental CO_2 concentration profiles measured inside the bed during the fast reaction period are interpreted with the KL fluid bed model, by supplying information on sorbent deactivation from laboratory tests. It is concluded that a fluidized bed of CaO can be a suitable reactor to achieve very effective CO_2 capture efficiencies from a combustion flue gas. © 2004 American Institute of Chemical Engineers *AIChE J,* 50: 1614–1622, 2004

Keywords: CO_2 capture, carbonation, fluidized beds, modeling, global warming.

Introduction

Increasing atmospheric concentration of CO_2, and concerns over its effect on climate, are powerful driving forces for the development of new advanced energy cycles, incorporating CO_2 capture and storage. It is generally accepted (Herzog, 2001) that the cost associated with the separation of CO_2 from flue gases introduces the largest economic penalty to this mitigation option. For current combustion systems, the only proven commercially available technology to separate CO_2 is based on amine-based absorption systems. However, this technology introduces severe efficiency penalties and added costs (Rao and Rubin, 2002), and this justifies a range of emerging approaches that claim to be more energy efficient and cost-effective than low-temperature absorption-based systems. One of these approaches (Silaban and Harrison, 1995) involves the separation of CO_2 at high-temperatures (>600°C) using the carbonation reaction of CaO

$$CaO\ (s) + CO_2\ (g) \rightarrow CaCO_3\ (s) \qquad T \text{ between } 650°C–850°C \text{ depending on pressure} \quad (1)$$

The background for this separation process dates back to 1867, when DuMotay and Marechal first patented the use of lime to aid the gasification of carbon by steam (Squires, 1967). The carbonation reaction can take place in a reducing atmosphere to enhance H_2 formation (Lopez-Ortiz and Harrison, 2002; Ziock et al., 2002; Lin et al., 2002; Areklett and Nygaard, 2002; Bandi et al., 2002; Wang et al., 2004), or in a combustion flue

Correspondence concerning this article should be addressed to J. C. Abanades at jcabanad@carbon.icb.csic.es.

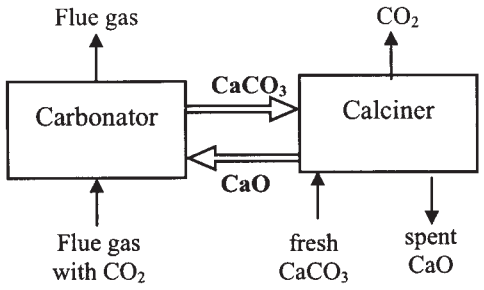

Figure 1. CaO carbonation-calcination cycle to capture CO_2.

gas (Shimizu et al., 1999; Abanades et al., 2003; Griffin et al., 2003; Wang et al., 2004). Figure 1 is a general scheme, common for all these options. The specific process configurations vary depending on conditions in the main units (temperature, pressure, reaction atmosphere, and fuel type), and on the method adopted to regenerate the sorbent by calcination, producing a concentrated CO_2 stream suitable for storage

$$CaCO_3\ (s) \rightarrow CaO\ (s) + CO_2\ (g) \qquad T > 900°C \text{ depending on pressure} \quad (2)$$

Shimizu et al. (1999) proposed the calcination of the sorbent by burning a fraction of the fuel in the calciner with O_2/CO_2. Other calcination options are under development to avoid the use of an air separation unit. For example, it has been proposed (Abanades et al., 2003) to use heat carriers, such as sintered CaO (particle density higher than 3,000 kg/m^3) circulating between a high-temperature combustion chamber and the calciner, where they are also separated from the sorbent (particle density below 1,800 kg/m^3) by segregation. Other indirect calcination options have been proposed by Ziock et al. (2002) and Griffin et al. (2003). In all these options virtually pure CO_2 can be obtained in the calciner, since no gas other than CO_2 (and steam if used to lower the partial pressure of CO_2, and the calcination temperature) can be produced from the calcination reaction.

Despite complexities in the regeneration step, there is an intrinsic benefit in using a high-temperature separation process for CO_2, when compared to low-temperature absorption or adsorption systems. In low-temperature systems, the heat delivered for sorbent regeneration cannot be efficiently recovered in the steam cycle, and the efficiency in a plant with CO_2 capture can be up to 40% lower than in a plant without capture (Rao and Rubin, 2002). In contrast, in systems using reactions 1 and 2, the energy used for calcination is recovered in the carbonator at temperatures still sufficiently high (higher than 650°C) for effective use in a steam cycle (Wang et al., 2004), or for enhancing endothermic reactions in the processes that follow the hydrogen generation route (Ziock et al., 2002). For the purpose of this work, we assume that at least one of these calcination options is available (for example, calcination in O_2/CO_2), and we can focus our interest on the carbonation process only.

There are two limits in terms of CO_2 capture efficiency from the gas phase in the carbonator. The first limit arises from the equilibrium in the carbonation-calcination reaction, which for the temperature interval of interest can be given by (Baker, 1962)

$$C_{CO2,eq} = \frac{1.462\ 10^{11}}{T} \exp(-19130/T) \quad (3)$$

This equilibrium allows for CO_2 capture efficiencies higher than 90% for typical coal combustion flue gases (12–15 vol % of CO_2) at atmospheric pressure and temperatures of around 650°C. However, the second and more important limit relates to the design of the carbonator as a chemical reactor. In principle, reactors with high throughput per unit area are essential to tackle the huge gas flows typical in large-scale power plants implementing a CO_2 capture system. Therefore, particles of CaO must react sufficiently fast, and to a sufficient extent to allow compact reactor designs. Bhatia and Perlmutter (1983) reviewed and investigated in detail the reactivity of CaO with CO_2, and reported a very rapid drop in the reaction rate after a given value of conversion, in agreement with many early studies. The diffusion mechanism that governs the slow reaction process after that critical conversion was studied by Mess et al. (1999), and has no practical interest from the perspective of a CO_2 capture device. Furthermore, these conversion capacities are limited by the decrease of the fast carbonation period, with the number of carbonation-calcination cycles, as shown by several early studies reviewed in a previous work (Abanades and Alvarez, 2003). To prevent this decay in activity, some methods are being proposed to manufacture improved $CaCO_3$ sorbents (Aihara et al., 2001; Gupta and Fan, 2002). However, these methods might overshadow one of the key advantages of methods following a lime carbonation-calcination route, since natural limestones are very cheap sorbents that allow for the large makeup flows contemplated in Figure 1.

Fluidized beds are a natural choice for carbonator reactors to capture CO_2, because of the high-reaction rates required, and the high enthalpy of the carbonation reaction. Fluidized beds have already been used in practice to capture CO_2 with CaO, operating at high pressure in the acceptor gasification process (Curran et al., 1967). However, there is no information available on the actual performance of a fluidized bed of CaO working as CO_2 absorber at the typical low CO_2 partial pressures of combustion flue gases. Therefore, the first objective of this work was to obtain experimental information from a small pilot fluidized bed of CaO (0.1 m i.d.), capturing CO_2 from a simulated combustion flue gas. The second objective was to interpret the results with a suitable mathematical model for the carbonator reactor by linking the existing information on sorbent performance at particle level, with a reasonable description of the gas-solid contact in the fluidized bed. Ultimately, it was our aim to show that a fluidized bed of CaO is a very effective device to capture the CO_2 emitted from power plants, hence, supporting the development of CO_2 capture concepts as outlined in Figure 1.

Experimental Studies

The pilot-scale mini-circulating fluid bed used in this work is presented in Figure 2. This has been described in detail elsewhere (Anthony and Lu, 1998), as a combustion unit and, therefore, only a brief description will be provided here. It

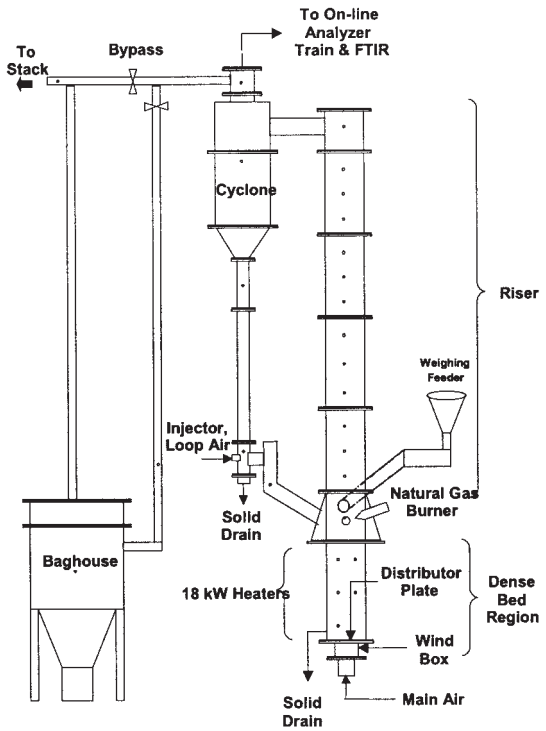

Figure 2. Pilot-scale fluidized-bed carbonator.

consists of a dense bed region, riser section, cyclone, and baghouse. The so-called dense bed region is 1 m high, and has an internal diameter of 100 mm. This section is also surrounded by four electric heaters (18 kW total), which can provide supplemental heat during operation. Heaters can maintain the dense bed region at a maximum temperature of 900°C. Air entering the dense bed region passes through a plenum or windbox, and is forced up through a distributor plate. Situated approximately 1 m above the distributor plate are the solid feed inlet port, return-leg port, and the natural gas burner. The natural gas burner is used to provide heat to the riser on startup. The riser has an internal diameter of 100 mm, is 5 m long, and is insulated with 75 mm of refractory. The mini-CFB is equipped with a data acquisition system, which records the system temperature, pressure drop, and gas composition. Temperatures in the dense bed region are measured at four different points by K-type thermocouples: 120, 240, 360, and 480 mm from the distributor plate. Thermocouples are also situated along the riser, cyclone, and return leg. The pressure drop in the riser is measured by a series of pressure taps. Gas sampling is performed at the top of the riser; detectors can record the levels of O_2, CO_2, CO, SO_2, and NO_x. Solid samples can be collected at the base of the return leg or via a valve immediately above the distributor plate in the dense bed region.

The carbonation-calcination tests conducted in this work were run in batch mode for the solids. They were initiated by loading 5 kg of limestone to form a bed of around 0.5 m height at minimum fluidization conditions. Two different limestones were used, Cadomin and Havelock, from western and eastern Canada, respectively. The CaO contents were 51.8 and 54.1, respectively, and the particle size ranges were between 650 and 1675 μm. The limestone beds were subjected to cyclic calcination in air at temperatures around 850°C, and carbonation at 650°C, with a synthetic gas mixture of air and 15% by volume of CO_2. The calcination part of every cycle was carried out by switching on the external bed heaters and allowing for a small flow of gas through the bed. There were 6 and 11 calcination-carbonation cycles completed for each limestone, similar to those presented in Figure 3 for the latest cycles with Havelock. During the calcination of Cadomin, only the electric heaters were used to supply heat to the fixed bed of solids. During the calcination of Havelock, a few short periods of fluidization were applied to mix the solids in the bed. The implications of this change in calcination conditions will be discussed below.

During the carbonation part of the experiments, the bed was fully fluidized at 1 m/s with a synthetic gas mixture of air and CO_2. The CO_2 concentration at the exit of the system showed that capture of CO_2 was very effective in these conditions, with values of CO_2 concentration apparently lower than equilibrium at the reference bed temperature under certain conditions. This was attributed to the residual recarbonation in the upper, cooler parts of the riser. Samples were collected after completion of the carbonation part of the cycle, which was clearly marked by a rapid increase in the CO_2 concentration profile (breakthrough) at the exit of the bed, as can be seen in the example of Figure 3. During some carbonation experiments, attempts were made to obtain in-bed CO_2 concentration profiles by sampling gas from the pressure taps (at 0.25, 0.37 and 0.5 m above the distributor), as shown in Figure 4.

Carbonated samples were collected after every calcination-carbonation experiment, and subjected to a range of techniques to aid in the interpretation of results. A scanning electron microscope (SEM, Zeiss DSM 942) was used for an examination of the internal structure of the carbonated sorbent particles and their calcines. In order to obtain fresh fracture surfaces for observation of the interior of the particles, the particles were lightly crushed by pressing between two pieces of glass, and the sample thus obtained was dispersed on a sticky graphite tab placed on an aluminum stub. The samples were gold-coated (~20 nm thickness) in order to improve the electronic signal, and also, to protect the surfaces from hydration and/or carbonation. The SEM images were formed from the backscattered electron signal, which normally yielded better quality pictures than the secondary electrons.

The textural analysis of the sorbents was performed using a mercury porosimeter (Micromeritics® AutoPore IV 9500)

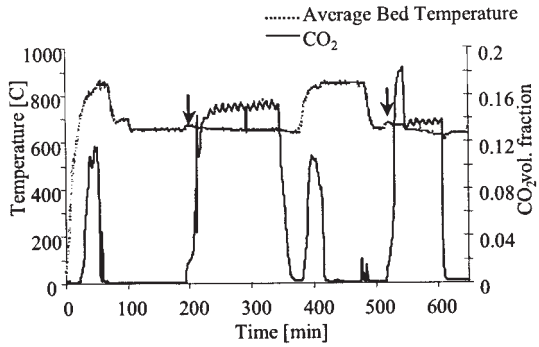

Figure 3. Havelock limestone cycles 10 and 11, carbonation at 15 vol. % CO_2 in air.

Note, arrows mark the onset of carbonation. Breakthrough times are better indicated in Figures 4 and 5.

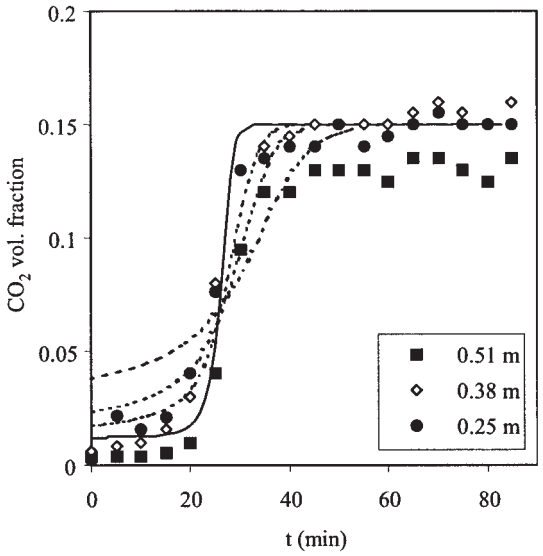

Figure 4. Experimental CO_2 concentrations measured at three different bed heights during a carbonation experiment (Cadomin limestone, cycle 1, 650°C, and 15 vol. % of CO_2).

Dotted lines correspond to model predictions at the same heights, and the solid line is at the exit of the bed.

which records Hg intrusion volumes in the pressure range 0.050–2250 bar (250 μm-5.5 nm pore dia.). Bulk densities were calculated from the Hg volume displaced at 1 bar; that is, regarding all the void space with diameter >12 μm, as interparticle cavities. Skeletal densities were in turn calculated from the Hg volume displaced at 2250 bar (5.5 nm pore dia.).

Results and Discussion

An example of a typical experiment is plotted in Figure 3 to show that during the carbonation part of the cycles, the bed of CaO efficiently absorbed the CO_2 fed to the system until a certain point (breakthrough), after which the CO_2 concentration rapidly climbed back to the value of the feed flue gas. Figure 4 shows the CO_2 concentration profiles measured from sampling ports located at different heights above the distributor (0.25, 0.37, and 0.5 m). As can be seen in these plots, the CO_2 has almost disappeared from the gas phase at expanded bed heights as low as 0.25 m. This was observed in all experiments at the beginning of the carbonation part of the cycles, where a sufficient amount of active CaO was present. These are encouraging experimental results because they show that, despite the deficiencies of gas-solid contact in the bubbling fluidized bed and the low-partial pressures of CO_2 in the feed-gas, the carbonation reaction is sufficiently fast at atmospheric pressure to allow compact reactor designs (reasonable throughputs per unit area of gas and reasonably low-bed heights). The detailed interpretation of these results (solid and dotted lines in Figure 4) will be discussed below.

From the solid-sorbent perspective, it was also obvious from Figures 3–5 that the bed of CaO reached a point of carbonation conversion well below unity, from which the amount of "active CaO" in the bed is no longer sufficient to retain the CO_2 entering the bed in the gas phase. This limited conversion $X_{b,N}$ was measured by sampling solids at the end of each carbonation cycle and measuring the weight-loss on calcination. In several series of experiments it was possible to confirm this conversion with a mass balance in the gas phase

$$X_{b,N} \cong \frac{M_{\mathrm{CaCO3}}}{W_0} \int_0^{\mathrm{end}} Q_g (C_{\mathrm{CO2},0} - C_{\mathrm{CO2,exit}}) dt \qquad (4)$$

The conversion at breakthrough decreased with the number of bed calcination-carbonation cycles as represented in Figure 6. As noted earlier, several studies on the reversibility of the carbonation reaction have reported a similar decay of maximum carbonation conversion with the number of calcination-carbonation cycles. We have developed a simple model at particle level to account for this decay (Abanades and Alvarez, 2003) that translates into the following semiempirical correlation

$$X_{b,N} = f_m^N (1 - f_w) + f_w \qquad (5)$$

According to this model, which qualitatively agrees with the carbonation mechanism outlined by Bhatia and Perlmutter (1983), $CaCO_3$ fills up all the available porosity made up of small pores plus a small fraction of the large voids, limited by the thickness of the product layer that marks the onset of the slow carbonation rate. Two model parameters ($f_m = 0.77$ and $f_w = 0.17$) reasonably fit many different series of data, and several of them were from other author sources. The reported data clearly suggested that the limestone type was not important to define $X_{b,N}$ in the first 20 cycles under conditions relevant for this work. Figure 6 shows this reference line together with the best-fit lines for the Cadomin ($f_m = 0.406$ and

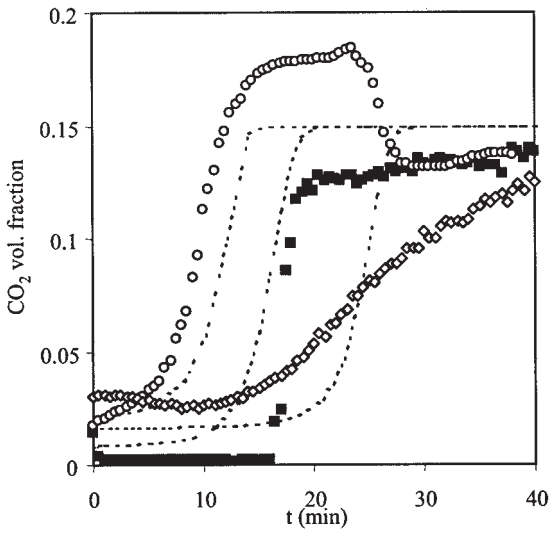

Figure 5. Experimental CO_2 concentrations measured at the exit of the bed in three different carbonation cycles (cycle 3, at 664°C, cycle 5 at 632 °C and cycle 11 at 672 °C) for the Havelock limestone.

Dotted lines correspond to model predictions at the exit of the bed under average carbonation conditions.

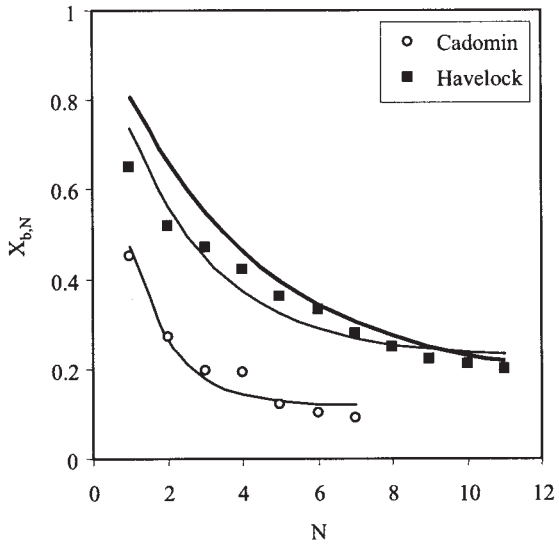

Figure 6. The decay in the CO_2 maximum carbonation conversion (end of the fast reaction period) vs. the number of carbonation-calcination cycles.

Solid lines are the best-fit curves to Eq. 3 of Havelock, Cadomin, and other limestones compiled in Abanades and Alvarez (2003).

$f_w = 0.117$) and the Havelock ($f_m = 0.658$ and $f_w = 0.226$) limestones. The Havelock bed data and its fitted constants are consistent with the trend of many other limestones and conditions represented by the thick solid line in Figure 6. However, the performance of the Cadomin limestone in the fluidized bed was much poorer than the general trend followed by Havelock and other limestones.

Figure 7 shows the SEM internal texture of the carbonated samples of Cadomin and Havelock after six calcination-carbonation cycles. A large difference in grain size between the Cadomin and Havelock calcines is apparent. Hg porosimetry data, not shown here, confirmed these large textural differences. Hg porosimetries of the calcines of several Cadomin samples taken from the bed after carbonation are plotted in Figure 8 against a calcine obtained in N_2 at 800°C from fresh Cadomin limestone. The huge textural differences between the calcines of samples from the bed and from the laboratory can only be explained accepting that, despite the nominally mild calcination conditions during the Cadomin tests (850°C in air), sufficiently strong sintering mechanisms were present during the first calcination cycle that yielded much poorer performance during the subsequent cycles, as shown in Figure 6. In contrast, the Havelock limestone seems to be more insensitive to bed calcination conditions. A further investigation of the sensitivity of sorbent performance to calcination conditions is in progress. For example, Curran et al. (1967) observed that the large differences in deactivation rates of different acceptors measured in a batch unit were not confirmed in the continuous unit, where calcination rates at the particle level were much higher. Despite these limitations of the Cadomin tests, both series of experiments will be used below to support the validation of a reactor model for the fluidized-bed carbonator.

A limitation of Eq. 5 is that it does not include the potential role of SO_2 in the flue gas as potential poison of the sorbent. In previous work, investigating these systems for high-sulfur fuels (Abanades et al., 2003), we have assumed that the active part of CaO will irreversibly be deactivated with the sulfur con-

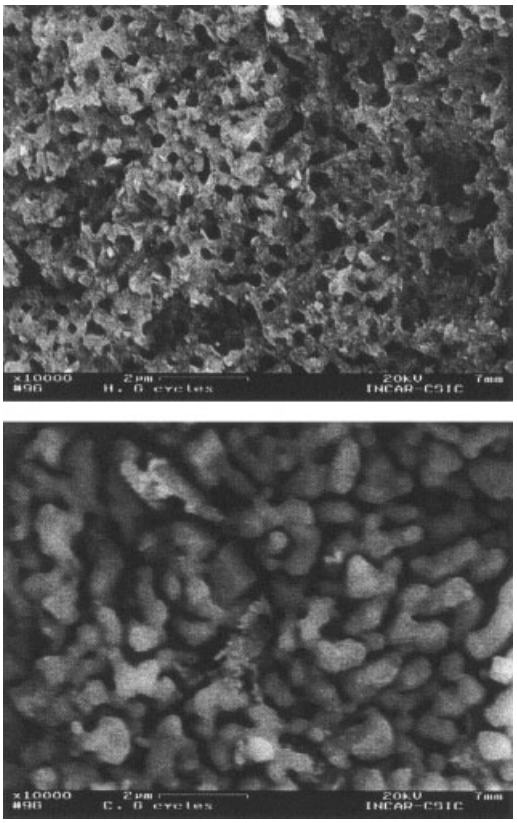

Figure 7. SEM micrographs of Cadomin (left) and Havelock (right) limestones after six calcination-carbonation cycles in the fluidized bed of Figure 2.

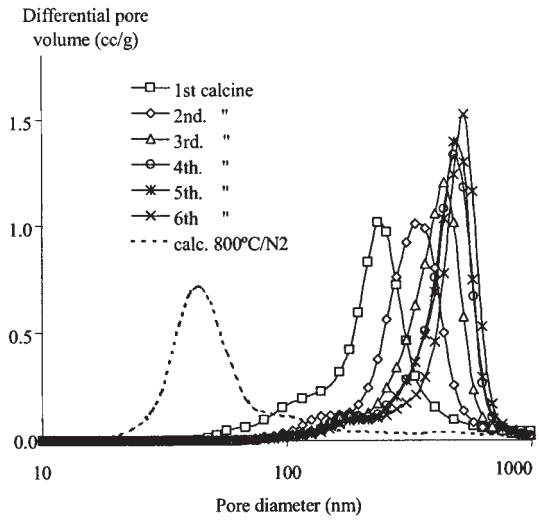

Figure 8. Pore-size distributions of Cadomin calcines obtained under mild calcination conditions (in N_2 at 800°C for the lefthand side curve) compared with those obtained from carbonated samples from the fluidized-bed tests.

tained in the fuel. However, since the molar C/S ratio is usually higher than 50, even in high sulfur-containing fuels, it can be shown that the average fractional conversion to $CaSO_4$ will be between 0.01–0.1, and this low level of conversion should not prevent the carbonation reaction of the remaining active CaO. A substantial increase in the sorbent makeup flow of Figure 1 is, however, required to compensate for the additional decay in activity originated by the presence of SO_2 in the flue gas. However, since Ca/S ratios will be very high under these conditions (>20), effective capture of SO_2 might be achieved in the carbonator units of these systems, avoiding the cost of desulfurization plants. No existing experimental evidence supports this claim.

Interpretation of experimental results from the fluidized-bed carbonator is attempted in the following paragraphs, using an idealized description of both sorbent performance at particle level, and gas-solid contact in the bubbling fluidized-bed carbonator. The general model proposed by Kunii and Levenspiel (1990) for bubbling fluidized beds has been adapted here to the conditions and characteristics of the experiments in the fluidized-bed carbonator. First, the fluidization conditions used during the tests (u = 1 m/s, average particle densities around 1,800 kg/m^3 and average particle sizes around 1 mm) clearly fall into the intermediate regime between "fast" and "slow" bubbles as defined by Kunii and Levenspiel (1990). Therefore, the bed is assumed to be divided into two phases: a bubble and an emulsion phase. To estimate the bubble fraction, we adopt a value proportional to the extremes proposed by Kunii and Levenspiel (1990) for the bubbling regime for fine and large-sized particles

$$\delta = \frac{u_0 - u_{mf}}{u_b + \dfrac{5u_{mf} - u_b\varepsilon_{mf}}{4}} \quad \text{for} \quad 1 < \frac{u_b\varepsilon_{mf}}{u_{mf}} < 5 \tag{6}$$

The gas entering the bed splits between these two phases and a CO_2 exchange is allowed among them (Kunii and Levenspiel, 1990). The superficial gas velocity u_0 changes slightly because of the removal of CO_2 from the gas phase and, therefore, an average value is adopted in these equations. The emulsion is assumed at minimum fluidization conditions. The effective gas velocity through the gas phase u_b^* is defined from the gas balance in a cross section of the bed

$$u_b^* = \frac{u_0 - (1 - \delta)u_{mf}}{\delta} \tag{7}$$

It is assumed that no solids are contained in the bubble phase and, therefore, all solids in the bed are contained in the emulsion phase. For any time during the initiation of the experiment, the bed contains three types of solids: a fraction of active CaO reacting in the fast reaction regime f_a, a fraction of inactive CaO from previous carbonation-calcination cycles 1-$X_{b,N}$, and a fraction of $CaCO_3$ given by the carbonation conversion X. Therefore

$$f_a = X_{b,N} - X \tag{8}$$

Knowing the fraction of CaO in the bed that is reacting in the fast reaction regime f_a allows the application of the KL model to estimate the CO_2 axial concentration profile. The KL model is formulated as a mass balance of CO_2 in the bubble and emulsion phases

$$-u_b^*\frac{dC_{b\mathrm{CO2}}}{dz} = K_{be}(C_{b\mathrm{CO2}} - C_{e\mathrm{CO2}}) \tag{9}$$

and

$$-(1 - \delta)u_{mf}\frac{dC_{e\mathrm{CO2}}}{dz} = (1 - \delta)(1 - \varepsilon_{mf})f_aK_r(C_{e\mathrm{CO2}} - C_{\mathrm{CO2eq}}) - \delta K_{be}(C_{b\mathrm{CO2}} - C_{e\mathrm{CO2}}) \tag{10}$$

The two critical parameters not yet defined in the previous equations are the reaction rate term K_r and the gas-interchange coefficient between phases K_{be}. Kunii and Levenspiel (1990) provide the following correlation for fluidized beds of the type used in this work (intermediate particle size)

$$K_{be} = 4.5\,\frac{u_{mf}}{d_b} \tag{11}$$

For the bubble diameter, the maximum bubble size d_b= 0.1 m has been adopted. Visual observation of the top surface of the bed gave evidence of "large" bubbles bursting there. Although, the average value of d_b should be below this number, d_b = 0.1 is a conservative assumption that yields the lowest value of K_{be}. Furthermore, the sensitivity of the model to K_{be} under the conditions tested (relatively deep fluidized bed) is low, affecting only the concentration data taken from the port located 0.25 m from the distributor, as will be seen later.

To define the reaction rate term K_r, we assume that the carbonation rate is first-order with respect to CO_2, and including the resistance to the mass transfer of CO_2 toward the particle of CaO in the emulsion phase, we have

$$K_r = \frac{1}{\dfrac{d_p}{6k_g} + \dfrac{1}{K_{ri}}} \tag{12}$$

This requires the definition of the CO_2 mass-transfer coefficient toward the carbonating particles k_g, which is estimated here with the correlation of Turnbull and Davidson (1984) for the Sherwood number

$$Sh = \frac{D_{\mathrm{CO2}}}{k_gd_p} = 2\varepsilon_{mf} + 0.95Re_{mf}^{0.5}Sc^{0.3} \tag{13}$$

To define the reaction rate constant for the carbonation reaction of the particles K_{ri}, we need to incorporate the key observations discussed in previous paragraphs. Therefore, we assume that K_{ri} = 0 after the particles reach the carbonation conversion limit $X_{b,N}$ that is estimated for each experiment with Eq. 5. It is also assumed that, in the active part of the conversion curves

(below $X_{b,N}$), the particle carbonates following the semiempirical equation

$$\frac{dX}{dt} = k_x X_{b,N}(1 - X)^{2/3}(C_{CO2} - C_{CO2,eq}) \tag{14}$$

This equation (except for the correcting term $X_{b,N}$, to account for the decreasing fraction of active CaO as the number of cycles increases) was found by early studies reviewed by Bhatia and Perlmutter (1983). These authors also noted that Eq. 14 is identical to the one obtained with the spherical grain model of Szekeley et al. (1976), consistent with our observations of the interior of the particles by SEM, if

$$k_x = \frac{k_s S_o}{(1 - e_o)} \tag{15}$$

The rate constant in suitable units for the KL model can be rewritten as

$$K_{ri} = k_s \frac{X_{b,N} S_0 \rho_{CaO}}{M_{CaO}} (1 - X)^{2/3} \tag{16}$$

We can adopt the reaction rate constant k_s as 5.95×10^{-10} m^4/smol, as measured by Bhatia and Perlmutter (1983) in conditions fully relevant for this work (temperature range between 673 and 998 K, and with CO_2 volume fractions between 0.1–0.42). For the surface areas of the fresh part of CaO of the calcines, values of $S_0 = 40$ m^2/m^3 and $e_0 = 0.5$ have been adopted for both limestones, yielding typical areas of 12 m^2/g of active CaO, consistent with data from Bhatia and Perlmutter (1983) for similar calcination conditions. With all these data, the particles achieve their maximum conversion $X_{b,N}$ in about 1 to 3 min. These times are in agreement with results reported by Bhatia and Perlmutter (1983), Silaban and Harrison (1995), or Shimizu et al. (1999) for the first calcination-carbonation cycle, and also agree with those obtained in the TGA with a different limestone in previous work (Abanades and Alvarez, 2003). Under these conditions, a fluidized bed with a sufficient amount of active CaO is a very effective CO_2 absorber, as became clear from the experimental results in Figures 3–5 and in the model predictions shown below.

With the previous assumptions and correlation to estimate the different parameters in the KL model, the CO_2 concentration profiles inside the bed can be calculated and compared with the experimental results of Figures 4–5. Since the carbonation reaction is assumed to be first-order, the analytical solution provided by Kunii and Levenspiel (1990) for Eqs. 9 and 10 yields the CO_2 axial concentration profile in the fluidized bed as

$$C_{CO2,z} = C_{CO2,eq} + \frac{(C_{CO2,0} - C_{CO2,eq})\delta}{(1 - \delta)u_o \Phi}[(1 - \Psi_2)(\Psi_1 \delta u_b^* + (1 - \delta)u_{mf})e^{-q_1 z} + (\Psi_1 - 1)(\Psi_2 \delta u_b^* + (1 - \delta)u_{mf})e^{-q_2 z}] \tag{17}$$

where

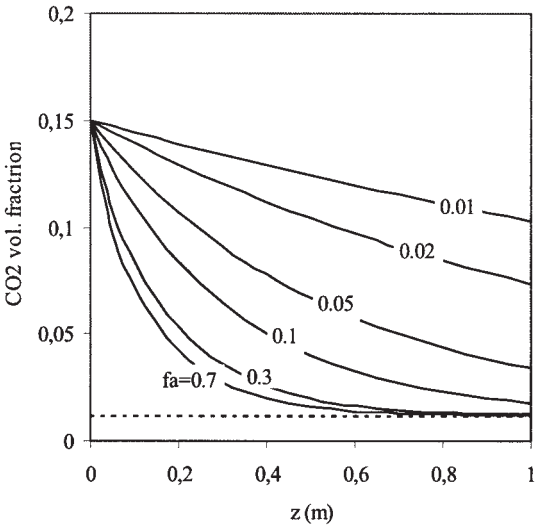

Figure 9. Effect of the fraction of active CaO present in the bed on the axial CO_2 concentration profiles as predicted by the model under average carbonation conditions used during the experiments (dp = 1mm, u = 1 m/s, T = 650°C, Wo = 5kg, 15 vol. % CO_2 in the gas feed).

$$q_1,\ q_2 = \frac{1}{2}\frac{f_a K_r}{u_{mf}}[1 - \varepsilon_{mf}] + \frac{1}{2}\frac{K_{be}}{u_{mf}}\left[\frac{\delta}{1 - \delta} + \frac{u_{mf}}{u_b^*} \mp \Phi\right] \tag{18}$$

$$\Psi_1,\ \Psi_2 = \frac{1}{2} - \frac{1 - \delta}{2\delta}\left[\frac{u_{mf}}{u_b^*} - \frac{f_a K_r}{K_{be}}(1 - \varepsilon_{mf}) \mp \Phi\right] \tag{19}$$

$$\Phi = \left[\left(\frac{f_a K_r}{K_{be}}(1 - \varepsilon_{mf})\right)^2 + \left(\frac{\delta}{1 - \delta} + \frac{u_{mf}}{u_b^*}\right)^2 + 2\left(\frac{f_a K_r}{K_{be}}(1 - \varepsilon_{mf})\right)\left(\frac{\delta}{1 - \delta} - \frac{u_{mf}}{u_b^*}\right)\right]^{1/2} \tag{20}$$

Figure 9 presents an example of the CO_2 concentration profile in the fluidized-bed carbonator calculated with Eq. 17, and the auxiliary equations above, for conditions resembling those used during the experiments. As can be seen in this figure, the CO_2 concentration profiles are insensitive to values of f_a higher than 0.1. This corresponds to the early stages in the carbonation cycle during the experiments where the emulsion phase is acting as a very effective sink for CO_2 and the overall carbonation process is controlled by the transfer of CO_2 from the bubble phase to the emulsion phase. With lower values of f_a, the concentration at the exit of the bed is appreciable, and this corresponds to the beginning of the breakthrough curves.

Simulated breakthrough curves corresponding to the experimental ones presented in Figures 4 and 5 can be estimated with the model by recalculating f_a as a function of time. This can be done by estimating the change of average carbonation conversion in the bed as

$$X = \frac{M_{CaCO3}}{W_0} \int_0^t Q_g (C_{CO2,0} - C_{CO2,exit}) dt \qquad (21)$$

The integration starts by calculating the concentration at the exit of the bed at the beginning of the experiment ($f_a = X_{b,N}$ for $t = 0$). This exercise was undertaken to produce the simulated CO_2 concentrations at the exit of the bed or at the bed-heights of the gas sampling ports that were included in Figures 4 and 5 as continuous dotted lines. As can be seen in these figures, there is reasonable agreement with the experimental results, when considering the number of simplifications and assumptions adopted to build the fluidized-bed carbonator model. It is important to emphasize that the sensitivity of these curves is low with respect to the assumptions and parameters adopted for the carbonation reaction rates at particle level, because the high reactivity of the fresh part of the CaO particles, at the conditions tested, is sufficiently large to guarantee a rapid change (both experimental and theoretical) in the CO_2 concentration at the exit of the bed in the proximity of the breakthrough conversion $X_{b,N}$ (defined with empirical Eq. 5).

The comparison between predicted and experimental CO_2 concentration data is poorer for the lower sampling ports (0.25 m above the distributor). While the model predicts significant concentration of CO_2 in the gas phase even at the beginning of the experiment (maximum f_a), all the experimental tests showed that, at the beginning of the carbonation period of each cycle, the bed was very effectively absorbing CO_2 even at this low sampling port. This discrepancy is due to the correlation adopted for the bubble-to-emulsion transport of CO_2 (Eq. 10) that seems to be too conservative for the actual bed conditions, since it does not allow more pronounced CO_2 concentration profiles, even when this transport is the only resistance to progress of the carbonation reaction in the bed. It is, however, beyond the scope of this work to refine this correlation for the limited number of fluidized-bed experiments conducted so far. It can also be noted that the breakthrough curves in Figure 5 show good agreement on the expected breakthrough times, but some differed from the model predictions in the shape of the CO_2 profile. As previously mentioned, recarbonation in cooler parts of the freeboard and some air leaks into the freeboard were detected in some carbonation tests. This explains why the intrinsic scattering of data seems higher in the experimental concentration of CO_2 measured at the exit of the riser (Figure 5) than in that CO_2 concentration measured inside and just above the fluidized bed (Figure 4).

Finally, it is necessary to highlight that, from a practical point of view, the most interesting part of the experiments and the model simulations are those with low values of f_a. This is because, in continuous carbonation-calcination systems to separate CO_2, it will be a design objective to maximize utilization of the sorbent and minimize losses of active CaO. Therefore, the value of f_a in a continuous operation must be kept low. For low values of f_a, the sensitivity of the model to the reactivity of the sorbent arising from the calcination is much more pronounced. Under these conditions, the general bed characteristics (superficial gas velocities, bed temperature, bed heights, bubble behavior, and so on) strongly affect performance of the fluidized-bed carbonator in terms of CO_2 capture efficiency in the gas phase. Despite these remarks, and in view of the results obtained so far, it has been shown that some attractive operating conditions exist where a fluidized bed of free CaO is an effective absorber of CO_2 from a combustion flue gas at high temperature.

Conclusions

Experiments in a small pilot fluidized-bed reactor have demonstrated that CO_2 capture from combustion flue gases can be effective at temperatures around 650°C. The key variable to understand the performance of the system as a CO_2 absorber is the fraction of CaO present in the bed reacting in the fast reaction regime. The amount of CaO available in the bed for fast reaction with CO_2 after each calcination-carbonation cycle decreases with the number of cycles. This decay in activity has been measured with two different limestones (Havelock and Cadomin). In the case of Havelock, the deactivation process is fully consistent with lab-scale results, and with a range of data reported by other authors. In contrast, differences observed in the Cadomin limestone are attributed to its different behavior at the specific calcination conditions during the calcination part of the cycles. Despite these differences between limestones, the experimental CO_2 concentration profiles, measured in the interior and at the exit of the bed during the fast carbonation period, show that the fluidized bed is an effective CO_2 absorber even after 11 cycles. The axial CO_2 concentration profiles during the carbonation part of the cycle have been interpreted with the KL model (Kunii and Levenspiel, 1990), adopting reactivity data from previous work and sorbent deactivation data from the laboratory tests. The model fits the available information reasonably well, but shows that more refined reaction models at particle level are required to predict reactor performance in beds with low fractions of active CaO. Despite these limitations, both the experimental and simulated results presented here show that a CO_2 capture process based on the carbonation reaction of CaO in a fluidized-bed reactor can be a solution to absorb, at high-temperatures, the CO_2 emitted from large combustion sources.

Acknowledgments

Part of this work is from a project partially funded by the European Coal and Steel Community (ECSC-7220-PR-125) and by the Panel on Energy Research and Development (PERD) in Canada.

Notation

$C_{bCO2,z}$ = CO_2 concentration in the bubble phase at height z, mol/m^3
$C_{CO2,0}$ = CO_2 concentration in the gas entering the bed, mol/m^3
$C_{CO2,eq}$ = equilibrium CO_2 concentration over CaO, mol/m^3
$C_{CO2,exit}$ = CO_2 concentration in the gas leaving the bed, mol/m^3
$C_{CO2,z}$ = CO_2 concentration in the gas at height z, mol/m^3
$C_{eCO2,z}$ = CO_2 concentration in the emulsion phase at height z, mol/m^3
d_b = bubble dia., m
D_{CO2} = effective gas diffusivity of CO_2 in air, m^2/s
d_p = particle dia., m
e_0 = particle porosity
f_a = fraction of CaO in the bed reacting in the fast reaction regime
$f_{m,w}$ = fitting constants in Eq. 5
k_s = rate constant for the carbonation reaction at the surface of CaO, m^4/s mol
k_g = mass-transfer coefficient of CO_2 toward the particles in the emulsion phase, m/s
k_x = effective reaction rate constant in Eq. 14
K_{be} = overall gas interchange coefficient between bubble and emulsion phases, s^{-1}

K_r = overall carbonation rate constant of particles in the emulsion phase, s^{-1}
K_{ri} = carbonation reaction rate constant, s^{-1}
M_{CaCO3} = molecular weight of $CaCO_3$, 0.1 kg/mol
M_{CaO} = molecular weight of CaO, 0.056 kg/mol
N = number of calcination/carbonation cycles
Q_g = total gas flow entering the bed, m^3/s
R = ideal gas constant, 8.314 J/mol K
Re_{mf} = particle Reynolds at minimum fluidization conditions
Sc = Schmidt number
Sh = Sherwood number
S_0 = initial surface area of CaO per unit volume of solid CaO, m^2/m^3
T = temperature, K
t = time, s
u_0 = superficial gas velocity, m/s
u_b = bubble rise velocity, m/s
u_b^* = effective gas velocity in the bubble phase, m/s
u_{mf} = minimum fluidization velocity, m/s
W_0 = mass of limestone loaded in the bed, kg
X = conversion of CaO to $CaCO_3$
$X_{b,N}$ = carbonation conversion at the end of fast reaction period in the N^{th} calcination/carbonation cycle
z = height from the distributor, m

Greek letters

δ = bubble fraction in the fluidized bed
ϵ_{mf} = bed porosity at minimum fluidization
ρ_{CaCO3} = true density of $CaCO_3$, 2710 kg/m^3
ρ_{CaO} = true density of CaO, 3310 kg/m^3

Literature Cited

Abanades, J. C., "The Maximum Capture Efficiency of CO_2 Using a Carbonation/Calcination Cycle of CaO/$CaCO_3$," *Chem. Eng. J.*, **90**, 303 (2002).

Abanades, J. C., J. E. Oakey, D. Alvarez, and J. Hämäläinen, "Novel Combustion Cycles Incorporating Capture of CO_2 with CaO," *Greenhouse Gas Control Technologies. Proc. of the 6th Int. Conf. on Greenhouse Gas Control Technologies*, Kyoto, Japan, J. Gale, and Y. Kaya, eds., Vol. I, Elsevier, Amsterdam, pp 181–186 (2003).

Abanades, J. C., and D. Alvarez, "Conversion Limits in the Reaction of CO_2 with Lime," *Energy and Fuels*, **17**, 308 (2003).

Abanades, J. C., D. Alvarez, E. J. Anthony, and D. Lu, "In Situ Capture of CO_2 in a Fluidized Bed Combustor,"*17th Int. Conf. on Fluidized Bed Combustion*, ASME, Jacksonville, FL, ASME, New York (2003).

Aihara, M., T. Nagai, J. Matsushita, Y. Negishi, and H. Ohya, "Development of Porous Solid Reactant for Thermal-Energy Storage and Temperature Upgrade Using Carbonation/Decarbonation Reaction," *Appl. Energy*, **69**, 225 (2001).

Anthony, E. J., and D. Lu, "Relationship Between SO_2 and other Pollutant Emissions from Fluidized Bed Combustion," *Proc. of the 27th Int. Conf. on Combustion*, A. R. Burguess and F. L. Dryer, eds., University of Colorado, Boulder, CO, 3093 (1998).

Areklett, I. and L. P. Nygaard, "Future Energy Plants," *Greenhouse Issues*, IEA Greenhouse Gas R&D Programme, 59 (2002).

Baker, E.H., "The Calcium Oxide-Carbon Dioxide System in the Pressure Range 1-300 Atmospheres," *J. Chem. Soc.*, **464,** 70 (1962).

Bandi, A., M. Specht, P. Sichler, and N. Nicoloso, "In Situ Gas Conditioning in Fuel Reforming for Hydrogen Generation," *19th Ann. Int. Pittsburgh Coal Conf. Proc.,* Pittsburgh Coal Conf., Pittsburgh, available in CD-ROM format with ISBN 1-890977-19-5 (2002).

Bhatia, S. K., and D. D. Perlmutter, "Effect of the Product Layer on the Kinetics of the CO_2-Lime Reaction," *AIChE J.,* **29**, 79 (1983).

Curran, G. P., C. E. Fink, and E. Gorin, "Carbon Dioxide-Acceptor Gasification Process. Studies of Acceptor Properties," *Adv. Chem. Ser.,* **69**, 141 (1967).

Griffin, T., A. Bill, J. L. Marion, and N. Nsakala, "CO_2 Control Technologies. Alstom Power Approach," Greenhouse Gas Control Technologies, *Proc. of the 6th Int. Conf. on Greenhouse Gas Control Technologies*, Kyoto, Japan, J. Gale and Y. Kaya, eds., Vol. I, Elsevier, Amsterdam, 81 (2003).

Gupta, H., and L. S. Fan, "Carbonation-Calcination Cycle Using High Reactivity Calcium Oxide for Carbon Dioxide Separation from Flue Gas," *Ind. Eng. Chem. Res.*, **41**, 4035 (2002).

Herzog, H., "What Future for Carbon Capture and Sequestration?" *Env. Sci. and Technol.*, **4**, 148A (2001).

Kunii, D., and O. Levenspiel, "Fluidized Reactor Models. 1. For Bubbling Beds of Fine, Intermediate, and Large Particles. 2. For the Lean Phase: Freeboard and Fast Fluidization," *Ind. Eng. Chem. Res.*, **29**(7), 1226 (1990).

Lin, S.Y., Y. Suzuki, H. Hatano, and M. Harada, "Developing an Innovative Method HyPr-RING to Produce Hydrogen from Hydrocarbons," *Energy Conversion and Management*, **43**(9–12), 1283 (2002).

Lopez Ortiz, A., and D. P. Harrison, "Hydrogen Production Using Sorption-Enhanced Reaction," *Ind. Eng. Chem. Res.,* **40**(23), 5102 (2001).

Mess, D., A. F. Sarofim, and J. P. Longwell, "Product Layer Diffusion during the Reaction of Calcium Oxide with Carbon Dioxide," *Energy & Fuels*, **13**(5), 999 (1999).

Rao, A. B. and E. S. Rubin, "A Technical, Economic and Environmental Assessment of Amine-Based CO_2 Capture Technology for Power Plant Greenhouse Gas Control," *Env. Sci. Technol.*, **36**, 4467 (2002).

Shimizu, T., T. Hirama, H. Hosoda, K. Kitano, M. Inagaki, and K. Tejima, " A Twin Fluid-Bed Reactor for Removal of CO_2 From Combustion Processes," *Trans. I. Chem.E.*, **77**- A, 62 (1999).

Silaban A., and D. P. Harrison, "High Temperature Capture of Carbon Dioxide: Characteristics of the Reversible Reaction Between CaO(s) and CO_2(g)," *Chem. Eng. Comm.*, **137**, 177 (1995).

Squires, A. M., "Cyclic Use of Calcined Dolomite to Desulfurize Fuels Undergoing Gasification," *Adv. Chem. Ser.*, **69**, 205 (1967).

Szekeley, J., J. W. Evans, and H. Y. Sohn, *Gas-Solid Reactions*, Academic Press, London (1976).

Turnbull, E., and J. F. Davidson, "Fluidized Combustion of Char and Volatiles from Coal," *AIChE J.*, **30**(6), 881 (1984).

Wang, J., E. J. Anthony, and J. C. Abanades, "Clean and Efficient Use of Petroleum Coke for Combustion and Power Generation," *Fuel,* **83,** 1341 (2004).

Ziock, H.-J., E. L. Brosha, F. H. Garzon, G. D. Guthrie, R, Mukundan, T. W. Robinson. B. Roop, B. F. Smith, A. A. Johnson, K. S. Lackner, F. Lau, E. J. Anthony, J. Wang, and J. Ruby, "Technical Progress in the Development of Zero Emission Coal Technologies," *19th Annual Pittsburgh Coal Conf.*, Pittsburgh, PA (2002).

Manuscript received July 10, 2003, and revision received Sept. 17, 2003.